

# “Aerogel-like” polysiloxane-polyurethane hybrid foams with enhanced mechanical and thermal-insulating properties

Letizia Verdolotti<sup>1</sup>, Maria Oliviero<sup>1</sup>, Marino Lavorgna<sup>1\*</sup>, Chiara Santillo<sup>1</sup>, Francesca Tallia<sup>2</sup>, Salvatore Iannace<sup>1</sup>, Shu Chen,<sup>2</sup> Julian R. Jones<sup>2</sup>

<sup>1</sup> Institute of Polymers, Composites and Biomaterials, National Research Council (IPCB-CNR), P.le E. Fermi 1, 80055 Portici (Na), Italy

<sup>2</sup> Department of Materials, Imperial College London, South Kensington Campus, London, SW7 2AZ, UK

## Abstract

New organic-inorganic polyurethane-based hybrids with enhanced mechanical properties and thermal insulation properties are reported. Polyurethane-based hybrids are characterized by the intimate interactions of their inorganic and organic co-networks and prepared by sol-gel approach, have exhibited properties exceeding those of polyurethane foams, e.g. enhanced thermal stability, durability and thermal insulating effectiveness. However, mechanical properties have previously been poor. Here, new porous organic-inorganic materials consisting of a polyurethane network modified by in-situ formation of aerogel-like polysiloxane domains, were developed. They exhibit a multiscale-porosity which enhances the insulation, mechanical and thermal properties. The synthesis was performed through a novel stepwise process consisting of: preparation of a siloxane precursor based on methyl-triethoxysilane and tetraethoxysilane; functionalization of traditional polyol for polyurethane foams with 3-(triethoxysilane)propylisocyanate as coupling agent; use of suitable catalysts and silicone surfactants; and foaming with methylene-di-isocyanate compound. The siloxane precursors and coupling agent led to formation of “aerogel-like” polysiloxane domains within the walls and struts of the polyurethane foams. The synthesis method enabled increased incorporation of the “aerogel-like” polysiloxane structures into the foams, compared to literature, with 20 wt% SiO<sub>2</sub>, reducing thermal conductivity of the hybrid foams 30% compared with pristine polyurethane, in addition to significant improvement in thermal stability and mechanical properties.

**Keywords:** Hybrid, Polyurethane Foam, Aerogel, Compressive Strength, Thermal conductivity

**\*Corresponding author:** Marino Lavorgna. email: [marino.lavorgna@cnr.it](mailto:marino.lavorgna@cnr.it)

## 1. Introduction

The environmental impact of manufacturing processes, energy consumption and energy waste on global warming is a huge challenge for scientific, political and industrial community. As reported by IEA (International Energy Agency) [1], the issue will continue to play a large and valuable role in the sustainable development of the global economy. Innovative materials may contribute significantly to reducing energy consumption in several sectors (buildings, transport, etc.). For example, in construction, it is possible to reduce the energy consumption, and cost, by designing adequately the materials for the building envelope (walls, roofs, floors, etc.), windows and thermal systems. However, reduction of energy waste still remains a challenge for the worldwide stakeholders involved in the supply-chain of insulating materials, also due to the increasingly challenging requirements driven by recent public energy policies [2]. Currently, thermal insulation materials suffer from various drawbacks, originating both from the manufacturing processes and the low sustainability of most of the raw materials used for their preparation. In fact, common insulating materials (such as polyurethane (PUR) foams, polystyrene foams, mineral fiber, inorganic foams, etc.) exhibit a thermal conductivity ( $\lambda$ ) value not lower than 24-46 mW/m K and their physical properties decline over time (environmental aging), increasing  $\lambda$  [3]. To overcome these technical limitations, several innovative solutions, such as the realization of vacuum within the porous materials enveloped in high barrier packaging or the production of nanoporous polymer foams or composite foams, have been widely investigated and some have translated to industrial applications [3-4]. However, the production of these solutions is expensive and additional problems may arise with anthropic action, e.g. the vacuum elements lose their superior insulation performance if the protective barrier packaging is accidentally pierced. Highly porous inorganic materials have emerged as thermal super-insulators, dielectric materials, reflective and anti-reflective coatings, flat-panel displays, sensors, catalyst supports etc. Silica aerogels are very promising mesoporous materials due to their high degree of porosity (>95%) [5], low-density ( $\rho$ : 0.003-0.5 g/cm<sup>3</sup>) and high specific surface area (500–1000 m<sup>2</sup>/g) [6], along with high thermal and acoustic insulation properties, low dielectric constant and low refractive indices [7-8]. Silica aerogels can be obtained by a silica gel, made by sol-gel, withstanding a drying process without reduction of the pore size in the gels as

the liquid phase is removed, usually via supercritical extraction (SCF) of the solvent [5]. This approach prevents the shrinkage of the network, which also minimizes the effect capillary forces that can cause cracking. However, the supercritical processing is expensive and incompatible with the processing requirements of many potential applications, e.g. size of components is limited by the size of the supercritical chamber. The high cost and their intrinsic brittleness have severely restricted the commercial exploitation of aerogels [8-9]. Nevertheless, efforts have been explored to improve the mechanical and functional properties of ScCO<sub>2</sub> aerogels to expand their market potential [7, 10]. In particular, the crosslinking with organic polymers and the modification of the surface area of aerogel with hydrophobic moieties have been explored [7,10]. To reduce the cost of drying, evaporative drying techniques that occur at room pressure and low or mild temperature, have also been exploited [5, 6, 7,10, 11, 12]. This gentle drying approach can result in xerogels [5, 10,13], as shrinkage occurs during the solvent removal, reducing pore size [5, 10]. Kanamori et al. [7,13] produced highly porous foams from methylsilsesquioxane via a solvent exchange process (water exchanged with a solvent with lower polarity), which were highly flexible, due to the presence of the two CH<sub>3</sub> groups producing hydrophobic chains. The functionality of these foams is limited as there are no side groups that can be targeted for functionalisation. Silicone-like materials are also susceptible to tearing. Recently, organic-inorganic (O-I) hybrid materials, which have co-networks of organic and inorganic components, have shown remarkable structural and functional properties and may represent a valid strategy to finally identify valuable substitutes of common polymeric foams. They can combine the properties of polymers, such as toughness [14-17] and elasticity, with those of the inorganic materials [15], including rigidity, high thermal stability, weathering and aging, improved gas barrier and chemical resistance [18]. These hybrids were generally obtained through a sol-gel process consisting of hydrolysis and condensation reactions of silane alkoxides to produce siloxane precursors as building blocks (at nanometric scale) that assemble to create a co-continuous networks with the polymeric chains [16]. This approach was used previously [17] to produce the first hybrid foam consisting of silica “aerogel-like” polysiloxane domains, consisting of primary silica particles (size around 2 nm) aggregated to form clusters structures, all embedded in the PUR network. The final product exhibited both a porous structure with micrometric cells, with average dimension around 200 μm, (closed pores associated to the foaming of the

polyurethanic matrix) and submicron sized domains dispersed in the walls and struts of foams, associated to silica-rich domains. These aerogel-like silica domains interacted with the polyol macromolecules through both weak interactions involving the oxygen atoms of the polyether moieties and covalent bonds due to the condensation of  $\text{-SiOH}$  from siloxane domains and HOR- groups from polyols. The presence of aerogel-like structures with their intrinsic porosity contributed to reducing the thermal conductivity of the foams. One reason the mechanical properties were poor was that it was not possible to produce reproducible foams with a silica content higher than 7 wt%, as the polymeric structure collapsed. The collapse was attributed to phase separation and the abundant hydro-alcoholic solvent molecules ( $\text{H}_2\text{O}$  and  $\text{CH}_3\text{CH}_2\text{OH}$ ) reacting with polyisocyanate molecules producing a high amount of  $\text{CO}_2$  gas. Another strategy was to add preformed silica aerogel nanoparticles into polyurethane foam matrices [8] but increasing the silica aerogel content from 0.5 to 1 wt% decreased the mechanical properties, due to the heterogeneous dispersion of nanoparticles. [17] Increasing the silica content further from 1 wt% to 5 wt% reduced thermal conductivity of the foams (0.0268 W/mK at 5 wt%), while the yield strain increased up to 5 wt% of silica content (more than 100% increment), but all the other mechanical properties (modulus, compression strength and Yield stress) decreased mainly when the silica content increased from 5 wt% to 7 wt%. They did not reach their theoretical mechanical properties due to lack of bonding between the components at the interface of the aerogel and polymer domains. Here, we report hybrid polyurethane/aerogel-like foams that show real synergy of the properties of the inorganic and organic components. This was achieved through creating hybrid foams of PUR and silica aerogel-like domains, with covalent coupling between the components, with a new synthesis approach that enables increased incorporation of the silica component. A stepwise approach was proposed: *a)* design and preparation of silica aerogel-like polysiloxane domains with tailored interfaces; *b)* functionalisation of the polyurethane precursor polyol with a coupling agent as 3-(triethoxysilanepropyl)isocyanate, IPTS, and mixing with the polysiloxane precursors; *c)* foaming by mixing the blend produced in the step *b)* with di-isocyanate (MDI) and optimal amounts of catalysts and silicone surfactant to control the kinetics of polyurethane synthesis and foaming. The produced hybrid foams were characterized in terms of chemical, morphological, mechanical and thermal properties.

## 2. Materials and Methods

### 2.1. Materials

Suprasec 2025 isocyanate (methylene-di-isocyanate, MDI,  $\eta = 400\text{-}800$  mPa\*s @ 25°C;  $\rho = 1.24$  g/cm<sup>3</sup> @ 25°C; average functionality: 2.85 eq/mole; NCO content: 29.7-31.3 %w/w) and polyether polyol (Daltolac R517,  $\eta = 6300$  mPa\*s @ 25°C;  $\rho = 1.093$  g/cm<sup>3</sup> @ 25°C) were kindly provided by Huntsman (Italy). Potassium acetate, CH<sub>3</sub>COOK and amine quaternary (PM40), used as catalysts for blowing and polymerization reactions respectively, and silicone surfactant (L6164) pore stabilizer were kindly provided by Momentive (Germany). TEOS (tetraethoxysilane), MTEOS (methyltriethoxysilane), HCl (hydrochloric acid, 2 M), ethanol (99.9%) and distilled water, used for the synthesis of the polysiloxane domains, and 3-(triethoxysilanepropyl)isocyanate (IPTS) used as coupling agent were supplied by Aldrich. All reagents were used as received unless noted otherwise.

### 2.2. Methods

#### 2.2.1. Preparation of polysiloxane precursor

The polysiloxane aerogel-like precursor was produced by sol-gel chemical approach by using two different experimental routes. In the first procedure (procedure A, Figure S1 of the “Supplementary Material”) a solution of TEOS (44 wt% with respect to the final solution), ethanol (39 wt%) and a solution of water (7.6 wt%) and HCl 2 M (0.5 wt%) were separately prepared and then mixed and stirred together at room temperature for 2 h; during this step the hydrolysis and condensation of TEOS takes place [17]. Then MTEOS (8.8 wt% with respect to the final solution) was added to the aforementioned solution and mixed at room temperature for additional 24 h; during this step MTEOS hydrolyzed and condensed with TEOS-based siloxane precursors. Once the mixing time was over, the hydroalcoholic solvents were partially removed, using a rotary evaporator, at 80 °C and 400 mbar, under vacuum at 50 rpm. In an alternative procedure (procedure B, Figure S2 of the “Supplementary Material”) TEOS (44 wt%), ethanol (39 wt%) and MTEOS (8.8 wt%) were mixed at room temperature for 15 minutes and then a solution of water (7.6 wt%) and HCl 2 M (0.5 wt%) was added and mixed at room temperature for further 24 h. In this stage, TEOS and MTEOS hydrolyzed and condensed simultaneously. Finally, the hydroalcoholic solvents were partially removed from the colloidal dispersions (through a rotary evaporator, at 80 °C and 400 mbar, under

vacuum at 50 rpm) obtaining the polysiloxane precursor as dense liquor. In both preparation processes, the obtained polysiloxane liquor was approximately 1/5 by weight of the initial hydroalcoholic mixture. The residual solvent, which was left in the liquor, was necessary to get the right viscosity and was used as blowing agent to promote polyurethane foaming.

### *2.2.2. IPTS functionalization of polyol, and preparation of blend polyol-IPTS functionalized polyol*

To improve the bonding between the polyurethane phase and the inorganic polysiloxane domains, the polyol-polyether was functionalized with a silane coupling agent (IPTS), such that 5% of OH groups of polyol reacted with IPTS. Polyol and silane are immiscible, but the presence of a phase-transfer catalyst, i.e. CH<sub>3</sub>COOK, allowed the formation of a homogeneous solution. This solution was stirred for 30 minutes at room temperature to obtain a complete reaction between OH and isocyanate groups. The obtained IPTS functionalized polyol was then mixed with pristine polyol to produce a “polyol blend” which in turn was used as raw material for the production of hybrid foams according to the composition reported in Table 1.

### *2.2.3. Preparation of hybrid PUR foams with polysiloxane aerogel-like domains*

The hybrid PUR foams with polysiloxane “aerogel-like” domains were produced starting from the polyol blends prepared with one of polysiloxane liquors (from procedures A and B reported in Figures S1 and S2 of the “Supplementary Material”, respectively). The polyol blend (formulated with 1 wt% of Niax PM40 catalyst, 1 wt% of Niax L6164 silicone surfactant and CH<sub>3</sub>COOK, 2 wt% of the polyol) were mixed at room temperature with different amounts of the polysiloxane liquors. These quantity of surfactants, catalysts and additives allowed fine control of the macroporous structure (i.e. foam density). Then, the aforementioned mixture was mixed with MDI (with NCO/OH ratio equal to 1.2), stirred for a few seconds and poured into a closed mold and left to react and foam for 1 h at room temperature (the scheme of the procedure for the preparation of hybrid foams is described in Figure S3 of the “Supplementary Material”). During the foaming step, the hydroalcoholic solvent still present in the initial precursor liquor was quickly vaporized due to the exothermic nature of the reaction, whereas aerogel-like structures formed, remaining entrapped in the walls of the PUR foam. The resulting hybrid foam samples were removed from the mold and stored for further characterization. Both a hybrid polyurethane sample without the IPTS functionalized polyol and a pristine polyurethane foam sample were also produced as controls. Table 1 reports the

formulation details of the foams obtained by using polysiloxane liquor produced by procedure B. The pristine polyurethane foam is labelled as PUR whereas the hybrid polyurethane foams are labelled as HPUR with the subscript “wca” is used to indicate the absence of coupling agents and the subscript “ca” to indicate the presence of polyol functionalized with IPTS coupling agent.

**Table 1.** Chemical composition of produced foams.

Sample	Polyol (%)	MDI (%)	f-polyol (%)	Polysiloxane liquor (%)	SiO <sub>2</sub> content from TEOS conversion (wt%) <sup>§</sup>	CH <sub>3</sub> SiO <sub>1.5</sub> content from MTEOS conversion (wt%) <sup>§</sup>
PUR	31.5	62.0	-	-	-	-
HPUR <sub>wca</sub>	24.7	49	-	24.7	18.32	5.83
HPUR <sub>ca1</sub>	24	48	3.58	24.7	18.32	5.83
HPUR <sub>ca2</sub>	20	47	5	27.4	20.27	6.47

<sup>§</sup>Theoretical silica content determined as SiO<sub>2</sub> from TEOS.

<sup>§</sup>Theoretical silica content determined as CH<sub>3</sub>SiO<sub>1.5</sub> from MTEOS

### 2.3. Chemical, morphological and functional characterization of materials

#### 2.3.1. Solid state Nuclear Magnetic Resonance spectroscopy (NMR)

Solid state <sup>29</sup>Si MAS-NMR characterization was performed for the identification the polysiloxane chemical structures present in the polysiloxane precursor sol just before their mixing with polyols blends. The sol was freeze-dried and then analyzed. Furthermore, NMR characterization was also used to investigate the chemical interactions between the polysiloxane and the PUR matrix. NMR spectra were collected by using a 600 Avanced Bruker spectrometer. <sup>29</sup>Si spectra where acquired by a 45° excitation pulse, 3280 scans, a spinning rate of 6 KHz and a recycle delay of 80 s. The top of sample rotor was filled with a small amount of 2,2-dimethyl-2-silapentane-5-sulfonic acid, DSS for frequency calibration. <sup>13</sup>C single pulse experiments where performed spinning the samples at 11 KHz, to reduce spinning sideband (SSB) superposition with sample resonances, and under proton decoupling co-adding 12K spectra with a recycle delay of 5 s.

#### 2.3.2. Small Angle X-ray Scattering (SAXS)

Structural characterization of PUR and hybrid materials was performed through Small Angle X-ray Scattering (SAXS) analysis using an Anton Paar SAXSess camera equipped with a 2D imaging plate detector. 1.5418 Å wavelengths CuK $\alpha$  X-Rays were generated by a Philips PW3830 sealed tube generator

source (40kV, 50mA) and slit collimated. Spectra of pristine PUR and hybrid foams were collected for 10 minutes. All scattering data were dark current and background subtracted, and normalized for the primary beam intensity [17,19].

### *2.3.3. Scanning Electron Microscopy (SEM) and Transmission Electron Microscopy (TEM)*

PUR and HPUR foams were cross-sectioned, gold coated with a sputter coater (Emscope SC500, UK) and analyzed by scanning electron microscopy (S440, LEICA) at an accelerating voltage of 20 kV or a Leo Gemini 1525 FEG-SEM, operating at 5 kV, with an InLens detector at a working distance of 6-9 mm and energy dispersive X-ray spectroscopy (EDS) to target the analysis of sample surfaces. The mean cell diameter was evaluated by Image J software (from NIH). A minimum of 50 for each sample were selected from micrographs and analyzed by assuming a spherical shape of cells. The nanostructure of the polysiloxane aerogel-like domains was analyzed by means of a Zeiss EM 902A transmission electron microscope (TEM). Ultrathin sections of the solid foam filled with epoxy resin were prepared and transferred onto copper grids and dried in open air for 2 h before microscopy. Morphological observations were carried out at an acceleration voltage of 120 kV.

### *2.3.4. Thermal analysis*

Thermo-gravimetric (TGA) analysis was performed, to evaluate the amount of silica content in the hybrid foams and the effect of silica amount on the thermal properties of the hybrid foams, using a TGA Q500 (TA Instruments, USA) over a T range from 30°C to 1000°C under air atmosphere. DSC analyses were performed to get insights about the glass transition temperature and the effect of inorganic phase on it. DSC was performed by using a Q1000, TA Instruments, USA. Samples were first heated from -80 to 180°C, then cooled to -80°C, and finally reheated to 180°C. The rate in both heating processes was 10°C/min.

### *2.3.5. Density measurements*

Sample density was calculated as the ratio between the weight and volume for a cubic specimen (2x2x2 cm<sup>3</sup>). The weight was measured by an analytical balance with a precision of 0.001 g and sample dimensions by a high-resolution caliper with an accuracy of 0.01 mm. The density value was expressed as average of densities values of four samples.



### 2.3.6. Thermal conductivity

Thermal conductivity,  $\lambda$  was measured according to EN12667 (thermofluximeter method). The instrument was Lasercomp Fox 314. The  $\Delta T$  between the two surfaces of foamed specimens was 10 °C (in details, the upper surface was at 10.02 °C and the bottom surface was at 20.01°C). The calibration material consisted of a glass fiber panel. The temperature was 22±3°C and the relative humidity was 50±10% HR.

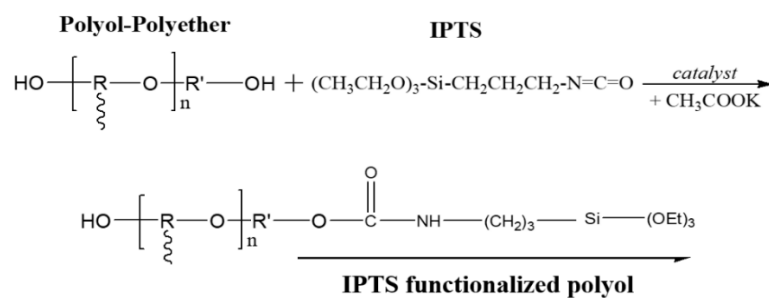
### 2.3.7. Mechanical properties

The mechanical properties of the foam specimens were investigated according to ASTM D 1621-04a protocol (Standard test method for compressive properties of rigid cellular plastics). The tests were carried out by using a dynamometer (Shenzhen Sans (China), model CMT 4304), equipped with a 1 kN load cell. Tests were performed at room T, by using specimen size 51 x 51 x 30 mm<sup>3</sup> and at crosshead velocity equal to 3.61 mm/min. Mechanical properties (compressive modulus and yield strength) were reported as average values of five tests for each material. The compressive modulus was calculated as slope of linear portion of the stress-strain curve [20]. The yield strength was obtained by means of the “tangent method”: the tangents to the elastic part and to the post-yield part were drawn in the stress-strain curve, and the ordinate of their intersection gave the compressive yield strength.

## 3. Results and discussion

### 3.1 IPTS functionalization of polyol

The occurring functionalization of polyol-polyether with IPTS was verified by FTIR analysis (Figure S4 of the “Supplementary Material”), in particular isocyanate functional groups of IPTS reacting with OH of polyol carried on urethane bonds through the reaction reported in the scheme 1:



**Scheme 1:** Functionalization reaction between polyol-polyether and IPTS to obtain IPTS functionalized polyol

### 3.2. Optimization of sol-gel process to produce hybrid foams

The hybrid foams were produced according two different routes: Procedure A, wherein the polysiloxane precursor was obtained by performing first the hydrolysis/condensation reactions for TEOS and then by adding MTEOS, which hydrolyzes and condenses on the pre-formed silica colloids; and Procedure B, wherein the polysiloxane precursor was obtained by performing the hydrolysis of TEOS and MTEOS simultaneously. This apparently small difference gives rise to hybrid foams with different properties. Hybrid foams produced according to Procedure A completely collapsed during the foaming process, whereas the hybrid foams produced according to Procedure B foamed well and foam production was reproducible. The different result is correlated with the structures of polysiloxane species produced by hydrolysis/condensation stages during the preparation of the liquor. [21] The species present into the polysiloxane liquors (obtained from Procedure A and B) were identified by  $^{29}\text{Si}$  NMR (Figure S5 of the “Supplementary Material”). Silica/siloxane nanoparticles formed from the hydrolysis and condensation of TEOS and as soon the MTEOS was added, hydrolyzed MTEOS species functionalized the dense silica colloids. Considering the notation  $Q_i^j$  and  $T_i^j$ , where Q refers to a silicon tetrahedral unit, and T is a C-Si-(OR)<sub>3</sub> unit, with  $i$  Si-O-Si covalent bonds, and  $j$  Si-OH bonds per unit [16, 21]), the liquor obtained from Procedure A had a higher content of fully condensed species (evidenced by NMR spectra showing mainly  $Q_4^0$ ) compared with the polysiloxane from Procedure B. Most OH groups present on TEOS-based colloids reacted with MTEOS species, therefore the polysiloxane from Procedure A had few available -OH groups to react with isocyanate groups. As soon as the polyisocyanate was added, the solvent molecules, mainly water and ethanol, reacted with the NCO groups, preventing a stable polyurethane network. The main consequence is that, by using the polysiloxane precursor produced through Procedure A, the foams collapsed, and they were not utilizable. The NMR spectra of the liquor from Procedure B (Figure S5 of the “Supplementary Material”) showed a higher amount of species with OH functional groups ( $T_2^1$ ,  $Q_2^2$ ,  $Q_3^1$ ), which were available to react both with isocyanate precursors and retain water through H-bonding interactions. The siloxane structure exhibited therefore a lower density, enabling the alcoholic solvent molecules to interact with -SiOH groups or fill hydrophobic pools made by the -CH<sub>3</sub> moieties of MTEOS. On the surface of the siloxane domains, water and ethanol molecules interact through large H-bonding network and are no longer easily accessible to react with the isocyanate molecules. This difference in the

structure of the siloxane species present in the two polysiloxanes liquors is of paramount importance and it controls the foaming reaction of PUR, avoiding the collapse of the structure when large amount of siloxane domains is used in the formulations. Therefore, the paper is focused only on the foams produced according to Procedure B.

### 3.3. Chemical characterization of the hybrid foams: NMR analysis

Figure 1 shows the  $^{29}\text{Si}$  MAS NMR spectra of hybrid foams obtained with and without coupling agent. The presence of  $Q_3^1$  and  $Q_4^0$  peaks, and the absence of  $Q_i^j$  species with  $i$  lower than 3, revealed that TEOS was fully hydrolyzed and condensed. The  $T$  resonance signals show a strong  $T_3^0$  peak (where  $T_i^j$  identifies species with Si atoms from MTEOS and IPTS with one Si–C bond,  $i$  siloxane bonds (Si–O–Si) and  $j=3-i$  hydrolyzed groups (Si–OH)) for the  $\text{HPUR}_{\text{ca}1}$ , which confirms a high condensations extent of hydrolyzed species originated from MTEOS and IPTS hydrolysis [16-18, 21-22].  $T_3^0$  and  $T_2^1$  resonance signals were, instead, simultaneously observed for the  $\text{HPUR}_{\text{ca}2}$  system. Thus, by increasing the polysiloxane liquor amount (and then theoretical siloxane content), the condensation T species reduced, as previously shown [16, 18, 21-22]. The presence of the coupling agent had a significant effect on the structure evolution since  $Q_3^1$  appeared significantly only when the IPTS functionalized-polyol was in the formulation. This may be ascribed to a selective condensation mechanism between  $Q$  species originated from TEOS and  $T$  species originated from IPTS, which, being more reactive than species originated from MTEOS for the presence of amine groups, react with  $Q_i^j$  species with  $i$  lower than 3, contrasting their condensation. In this way, the resulting siloxane network becomes more open and less condensed. The high –OH content allows binding of hydroalcoholic solvent molecules and avoids their reaction with isocyanate groups [16-17, 21-22].

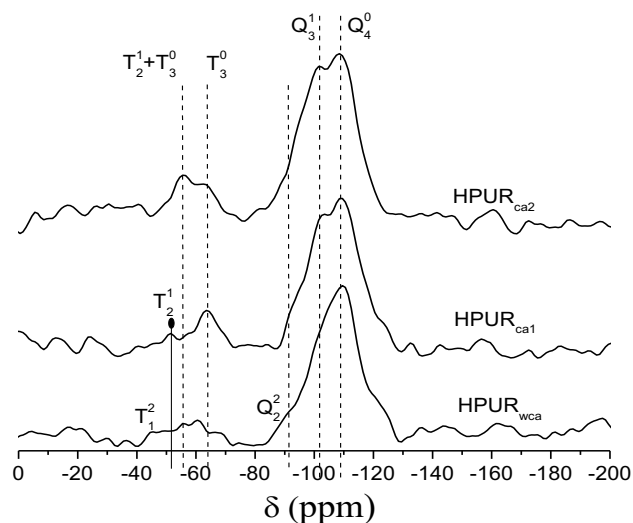


**Figure 1.**  $^{29}\text{Si}$  MAS NMR of hybrid polyurethane foams:  $\text{HPUR}_{\text{wca}}$ ,  $\text{HPUR}_{\text{ca1}}$  and  $\text{HPUR}_{\text{ca2}}$ .

#### 3.4. Morphological characterization: SAXS, SEM and TEM analysis

The morphology of hybrid foams and the morphology of polysiloxane aerogel-like domains embedded into cell walls and struts was observed by SEM and TEM analysis. The SEM images of the cross-section surface of pristine PUR and hybrid foams at low and high magnification are shown in Figure 2 and 3, respectively. Low magnification images (Figure 2) show that foams were successfully produced. The SEM images of pristine PUR (Figures 3a) and 3b)) show, as expected, a smooth cell surface. On the contrary, the SEM images of  $\text{HPUR}_{\text{ca2}}$  (Figures 3c), 3d) and 3e)) show the presence of nanostructured polysiloxane domains, which appeared in the cross-section of struts and within the cell walls. These domains were constituted by agglomerates of spherical silica particles (as observed in the EDS analysis reported in “Supplementary Material” Figure S6) and were homogeneously distributed to produce a network entrapped in the polymeric matrix, as observed in the SEM micrographs (Figure 3d)). Furthermore, Figure 3e) shows the SEM image of aerogel-like siloxane domains, which result from aggregation of small and uniform particles, densely packed to realize nanoporous structures. SAXS measurements (Figure S7 of the “Supplementary Material”) revealed additional information on the hierarchical structure of the polysiloxane domains. Indeed, by applying the Guinier's law, [23] is found that polysiloxane domains in  $\text{HPUR}_{\text{ca1}}$  and  $\text{HPUR}_{\text{ca2}}$  samples are characterized by primary polysiloxane particles with a radius equal to 1.9 and 2.1 nm respectively.

Furthermore, SAXS curves of hybrid foams show a slope in the Porod region of 2.6-2.7 indicating that primary polysiloxane particles aggregate to form the spherical fractal aggregates observed by SEM analysis.

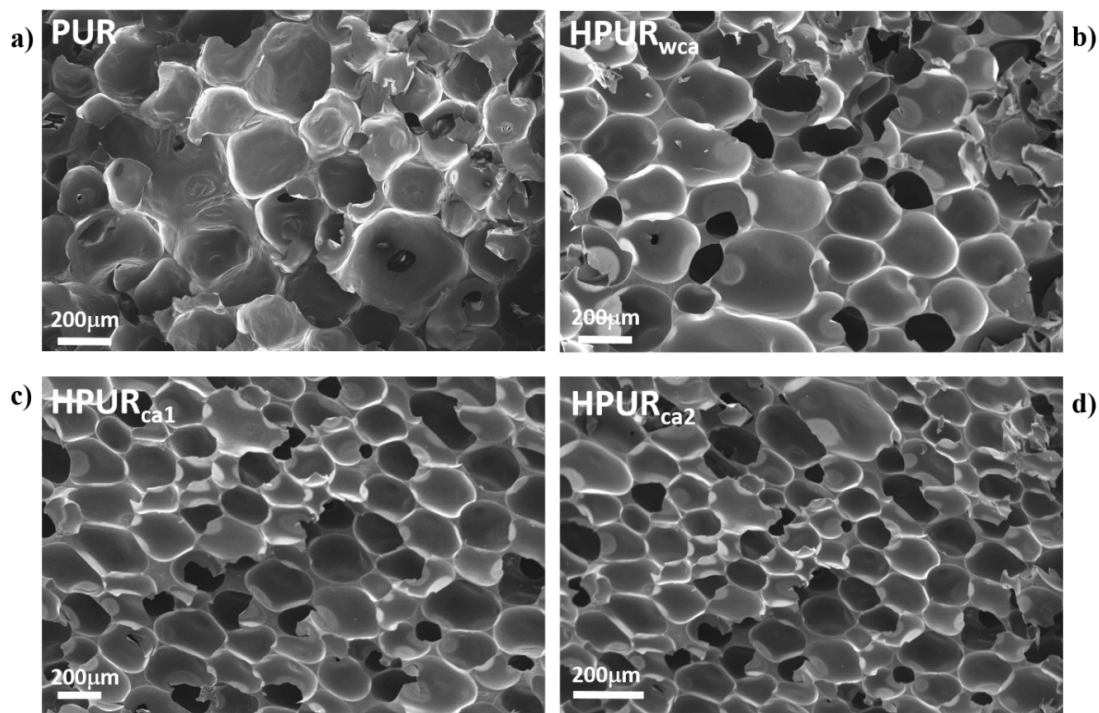


**Figure 2.** SEM images at low magnification of a) pristine polyurethane foam, PUR @ Mag=150X; b) hybrid polyurethane foam, HPUR<sub>wca</sub> @ Mag=65X; c) hybrid polyurethane foam, HPUR<sub>ca1</sub> @ Mag=55X; d) hybrid polyurethane foam, HPUR<sub>ca2</sub> @ Mag=50X.

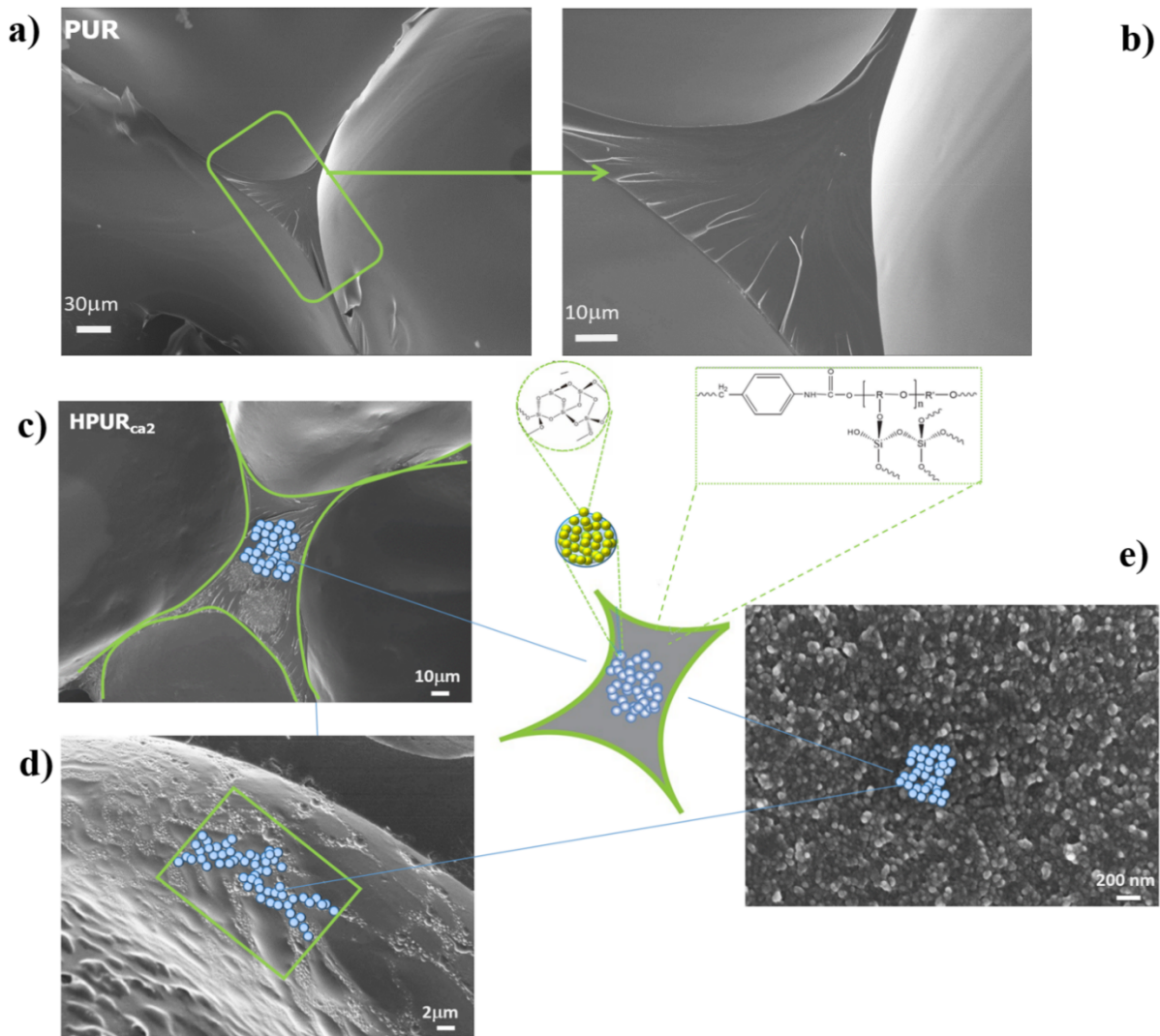


**Figure 3.** SEM images of foams at high magnification: a) pristine polyurethane foam, PUR @ Mag=700X; b) pristine polyurethane foam, PUR @ Mag:2.56 kX; c) hybrid polyurethane foam HPUR<sub>ca2</sub> @ Mag=1.2 kX; d) hybrid polyurethane foam HPUR<sub>ca2</sub>, @ Mag=7.45 kX; e) silica aerogel located within the pore walls the hybrid polyurethane foam, namely HPUR<sub>ca2</sub>, @ Mag=114.7 kX

These outcomes are confirmed by TEM observations too (Figure 4), in which the polysiloxane domains homogeneously distributed in the polymer matrix (within the cell walls and struts of PUR) can be observed. Polysiloxane nanoparticles (with diameters of approximately 130 nm) were identified embedded in the polymeric matrix. Figure 5 shows cell diameter distributions for pristine PUR and HPUR foams, from SEM analysis. Adding polysiloxane domains (HPUR<sub>wca</sub>) to the polymer matrix (PUR), caused a small decrease in the mean cell diameter (the cell diameter increased from 320 to 280 μm). The presence of coupling agent (HPUR<sub>ca1</sub>) significantly decreased the mean cell diameter, and increasing the amount of coupling agent (the

$f$ -polyol increased from 3.58% for HPUR<sub>ca1</sub> to 5% for HPUR<sub>ca2</sub>) caused a further decrease (the cell diameter decreased to 160 and 120  $\mu\text{m}$  respectively by increasing the content of coupling agent). A significant reduction of about 60% in the mean cell diameter was observed for the sample HPUR<sub>ca2</sub> with respect to pristine PUR. The small decrease in pore size due to polysiloxane addition (without coupling agent) confirms that the cell diameter does not depend on the polymer dilution with the siloxane phase. The larger decrease in cell size due to coupling agent addition was due to the coupling agent improving covalent bonding between polysiloxane domains and PUR matrix and it disrupting the siloxane network, as confirmed from the  $^{29}\text{Si}$  NMR results. The nucleation rate of cells during PUR foaming is known to increase significantly as cell size decreases and smaller cells result in increased homogeneous morphology [24-25]. The improvement in cell nucleation promoted by polysiloxane was not observed for the system without coupling agent (the mean cell diameter of HPUR<sub>wca</sub> foam was only ca. 9% smaller than the mean cell size of pristine PUR). This result may be ascribed to the high aggregation of polysiloxane nanoparticles in absence of coupling agent, which reduces the efficiency of the surfactants, causing heterogeneity of nucleation. This is confirmed also by TEM analysis (Figure 4), where for the system without coupling agent, coarse polysiloxane domains (in the range of 1  $\mu\text{m}$  diameter) were detected in the hybrid alongside with smaller particles.

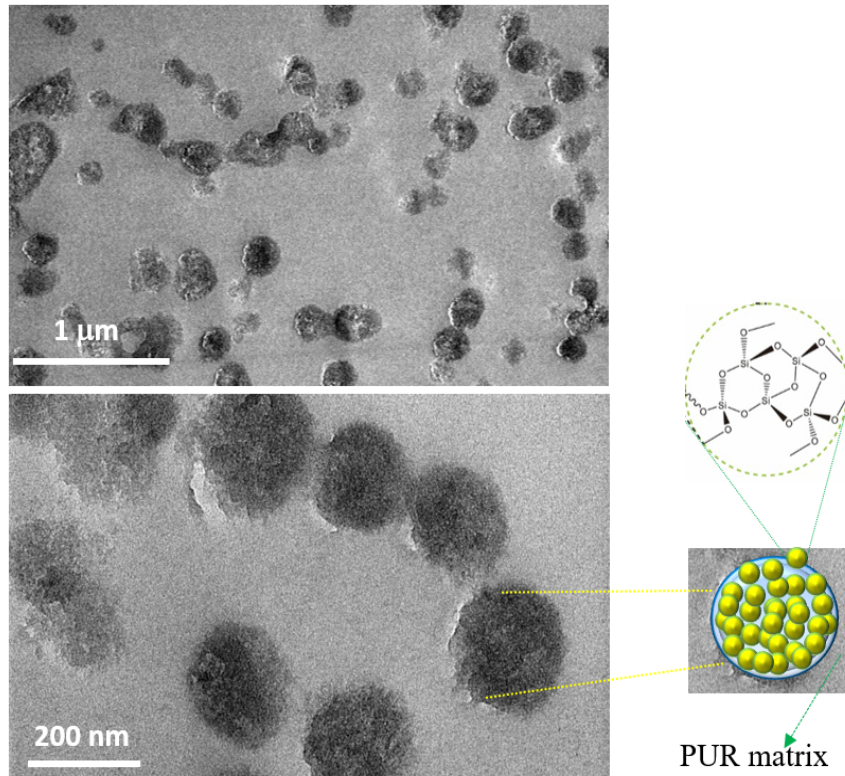


**Figure 4.** TEM images of siloxane domains present in hybrid polyurethane foam HPUR<sub>ca2</sub>.

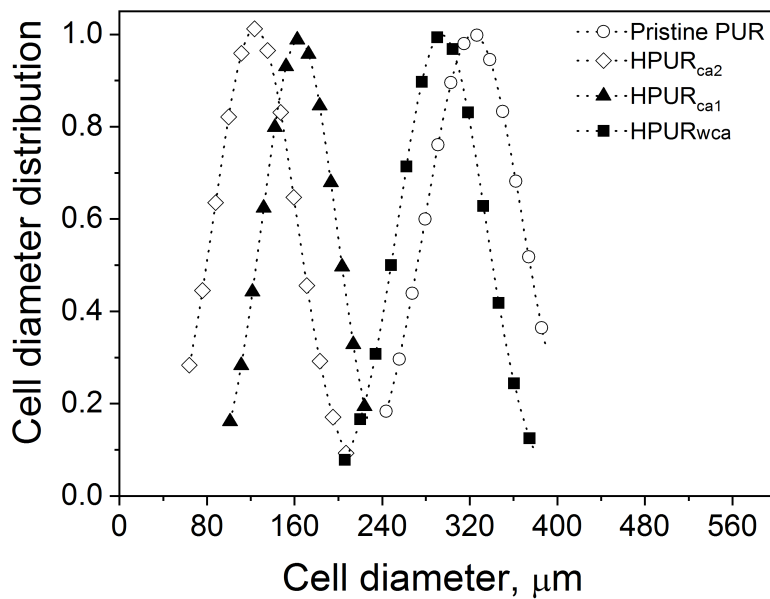


**Figure 5.** Normal distributions of cell diameter of the pristine polyurethane foam, PUR and hybrid polyurethane foams (namely HPUR<sub>wca</sub>, HPUR<sub>ca1</sub> and HPUR<sub>ca2</sub>) determined from analysis of SEM images.

### 3.5. Physical characterization: thermal conductivity and thermal (TGA/DSC) analysis

Results of thermal properties by TGA and DSC analysis are summarized in Table 2. Generally, polyurethane foams show three thermal degradation processes [19, 26, 27]. In the 120–300 °C range (the



maximum temperature of the weight loss derivative is namely  $T_{\max 1}$ ) the detected weight loss is generally very low and correlated to the evaporation of small molecules. In the case of hybrid foams the weight loss in this temperature range is ascribed to the completion of condensation reactions and loss of adsorbed solvent molecules [17]. The second degradation step which occurs in the range of 300–350°C ( $T_{\max 2}$ ) is assigned to the oxidative reactions of urethane bonds, which generate polyol segments, isocyanate and secondary complex products, and also combustion volatiles compounds. The secondary complex products degrade at high temperature ( $>450^\circ\text{C}$ ,  $T_{\max 3}$ ). [19, 27, 28]. As reported in Table 2, the maximum decomposition temperatures of the hybrid foams, mainly  $T_{\max 2}$  and  $T_{\max 3}$  increased with the addition of polysiloxane as compared with pristine PUR; this improvement in thermal stability can be ascribed to the presence of polysiloxane domains which protect the polyurethane phase from thermal degradation and shield it from action of thermal oxidative gases [17]. Moreover, the silica content was identified as residue at 1000°C and resulted to be 20 wt% for the HPUR<sub>ca2</sub>. The glass transition,  $T_g$  increased as the polysiloxane content increased, as the silica constrained the molecular relaxation of polyurethane macromolecules [16]. The  $T_g$  increased significantly for the systems with the IPTS functionalized polyol, characterized by the larger amount of aerogel-like particles and smaller and more well-dispersed particles, due to the contribution of silica/siloxanes of the coupling agent, which probably realize a more extensive interpenetrating network, acting as a better physical constraint to contrast the molecular relaxation. In fact, the HPUR<sub>ca2</sub> had a  $T_g$  which was almost 20°C higher than that of HPUR<sub>wca</sub> (without coupling agents), which was characterized by the presence of coarse polysiloxane domains. The thermal conductivity,  $\lambda$ , of the foams (Table 2) decreased as polysiloxane content increased, up to reduction of 37.5% for HPUR<sub>ca2</sub> compared to the pristine PUR foam. This is in agreement with results reported in the literature for foamed systems modified with aerogel, mainly preformed, particles (in amount ranging from 0.5 wt% to 8 wt%) [4, 8, 17, 24, 29]. The thermal conductivity of a foam material is given by a combination of several contributions [24, 30-32]:  $\lambda_i = \lambda_s + \lambda_g + \lambda_r + \lambda_c$  where  $\lambda_s$  corresponds to the conduction through the solid phase (cell walls),  $\lambda_g$  to the conduction through the gas-filled inside the cells,  $\lambda_r$  is the heat radiation through the cell walls and  $\lambda_c$  (negligible for cell size smaller than 4 mm [17, 30, 32]) is related to the convection within the cells. To reduce the overall thermal conductivity,  $\lambda_i$ , at least one of the aforementioned contributions

has to reduce. The reduction of the thermal conductivity with the polysiloxane content is known to be ascribed to both: 1) the reduction of the cell size due to nucleating effect of polysiloxane domains and 2) to the embedding of aerogel-like structures within the cell/struts of polyurethane matrix, reducing  $\lambda_s$  [17].

**Table 2.** Thermal properties of produced polyurethane foams

Sample	T <sub>max1</sub>	T <sub>max2</sub>	T <sub>max3</sub>	Residue at 1000°C, wt% SiO <sub>2</sub>	T <sub>g</sub> (°C)	$\lambda$ (W/mK)
Pristine PUR	316	330	560	0	24.5	0.04
HPUR <sub>wca</sub>	273	314	561	17	40	0.032
HPUR <sub>ca1</sub>	215	335	570	17.8	49.1	0.028
HPUR <sub>ca2</sub>	267	340	620	20	59.2	0.025

### 3.6. Mechanical characterization

Figure 6 shows the stress–strain curves obtained from compressive tests of pristine PUR and HPUR foams. The HPUR<sub>ca1</sub> and HPUR<sub>ca2</sub> foams exhibited higher stiffness and yield strength compared to pristine PUR (Figure 6) and also compared to hybrid foams reported by authors in a previous work [17]. For the hybrid foams of our previous work [17], the presence of silica domains (at different percentages to 1.5 wt% up to 7 wt%) led to a reduction of the mechanical properties with respect to the pristine PUR, which was ascribed to the higher amount of hydroalcoholic solvent molecules of polysiloxane liquor, that induced undesired reactions with isocyanate and discontinuity of the polymeric structure during the foaming process, and also to the absence of a bonding between the polymeric phase and siloxane domains. In this study, the use of formulations of polysiloxane precursors with well-balanced hydrophobic and hydrophilic properties alongside the role of the coupling agent permitted production of hybrid PUR foams which did not collapse during the foaming process. The stiffness and yield strength of the resulting HPUR<sub>ca</sub> foams increased as the percentage of polysiloxane domains increased. In the case of the hybrid foam without coupling agent, HPUR<sub>wca</sub>, a decrease of both stiffness and yield strength was, instead, observed with respect to pristine PUR foam. To justify this, we should consider the effects of polysiloxane domains and of coupling agent on factors such as hydrogen bonds, covalent bonds and cellular structures [24, 32]. The overall effects of polysiloxane domains, with or without coupling agent, on mechanical properties of PUR foam depend on: a) the positive effects of silica aerogel in reinforcing the polyurethane matrix and the cellular structures; b)

negative effects of silica aerogel in disrupting the hydrogen bonds network which is well-established in the polyurethane phase [33]. Mechanical properties such as Young's modulus ( $E$ ) and yield strength ( $YS$ ) are given in Table 3. In the same table are, also reported the densities of the corresponding foams. Considering the strong influence of foam density on foam compressive properties, specific values of the mechanical parameters (specific compressive modulus,  $E^*$  and specific yield strength,  $YS^*$ ) were calculated by normalizing the values of mechanical properties to the foam density. The addition of aerogel-like siloxane domains to the polyurethane formulation led to improved mechanical behavior of hybrid foams  $HPUR_{ca1}$  and  $HPUR_{ca2}$  with respect to the pristine PUR. For instance,  $E^*$  increased with increasing of the amount of polysiloxane domains, i.e. around 211% and 387% respectively for  $HPUR_{ca1}$  and for  $HPUR_{ca2}$  foams, furthermore an increase of 120% in  $YS^*$  for  $HPUR_{ca2}$  is also recorded. This result is in agreement with the change on the resulting foam morphologies, which were characterized by cells with lower dimensions (Figure 2 and Figure 5). Smaller cells caused the stress applied to the polyurethane matrix to be distributed between a greater number of cells and, therefore, the overall tolerance of polyurethane foam increased against the stress. In addition to the change in morphology, these outcomes highlight the important role of coupling agent that is able to create an effective covalent interface between the polyurethane matrix and the aerogel-like siloxane domains, with consequent increase of the foam stiffness. Similar results were obtained for rigid composite foams polyurethane and nanosilica modified with n-(2-amonoethyl)-3-aminopropyltrimethoxysilane [34], with the improvement of static mechanical properties attributed the to the formation of additional covalent bonds and more interfacial interactions in the boundary layer. On the contrary, the compressive response of the hybrid foam without coupling agent,  $HPUR_{wca}$ , shows a negative effect of silica domains addition for  $E^*$  and  $YS^*$  parameters. This behavior can be attributed to the poor adhesion between the filler and polymeric matrix where, as indicated by TEM analysis, polysiloxane domains were coarse. Thus, an interruption of continuity of polymeric matrix (disruption of formation of hydrogen bonds) can occur, leading to defects and cracks responsible of the reduction of  $E^*$  and  $YS^*$  [35]. Although the  $HPUR_{wca}$  sample shows a mean cell size slightly lower than those of PUR foam, it had lower  $E^*$  and  $YS^*$  values compared to the pristine PUR foam. Figure 7 shows a graph of normalized Young's modulus as a function of the inorganic content (filler) for hybrid foams with coupling agent,  $HPUR_{ca1}$ ,

HPUR<sub>ca2</sub> and the mechanical properties of other polyurethane nanocomposite rigid-foams, with various filler materials, from literature. In particular systems with various contents of different fillers are considered: Silica Aerogel (SA) [8, 17, 24], Multiwall Carbon Nanotubes (MWCNTs) [36], Surface Modified Montmorillonite Clay (SM MMT-Clay) [37], Lignin (Lign.) [38], Cellulose Fibers (CFs) [39], Flax Fibers (FFs) [40] and Pineapple Leaf Nanofibers (PLNFs) [41]. The effect of filler content on the  $E^*$  was also evaluated, and it was calculated as ratio with respect to the pristine materials, namely relative  $E^*$ :  $E_r^*$ . The data confirm the efficiency of different analyzed fillers to enhance the mechanical properties of polyurethane foams. However, it is clear that the mechanical properties of nanocomposites foams of literature are greatly influenced by the aggregation behavior of fillers. The  $E_r^*$  values of these foams, in fact, decreased or did not change as filler content increased above a certain value. On the contrary, the presence of coupling agent in the HPUR<sub>ca1</sub> and HPUR<sub>ca2</sub> foams improved the dispersion of filler in the matrix, also, at higher filler content, offering a significant improvement of mechanical behavior. Finally, Table 3 presents a comparison of hybrid foam with the highest content of polysiloxane domains, i.e. HPUR<sub>ca2</sub>, with commercial PUR foam for thermal insulation, produced with DALTOFOAMTR-33256. The parameters used for the comparison are the compressive strength and thermal conductivity. Since the thermal conductivity is also a function of foam density, specific parameters (specific compressive strength,  $CS^*$  and specific thermal conductivity,  $\lambda^*$ ) were calculated by normalizing the values of these properties to the foam density. It is evident that the developed hybrid foam HPUR<sub>ca2</sub> exhibits both better mechanical and thermal-insulating properties than the commercial PUR foam, and for this reason, it is a valuable candidate in building applications.

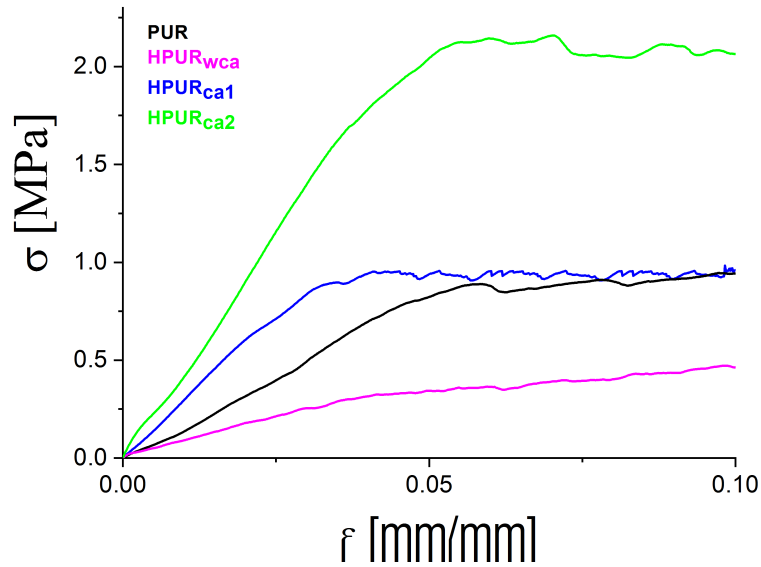


**Figure 6:** Representative stress-strain curves of PUR and HPUR foams.

**Table 3:** Compressive properties and bulk density of PUR and HPUR foams. YS is the yield strength and E is the Young's modulus. YS\* and E\* are specific mechanical parameters, calculated by normalizing the values of mechanical properties to the foam density.

Sample	Density (kg/m <sup>3</sup> )	YS (MPa)	E (MPa)	YS* (MPa/ kg/m <sup>3</sup> )	E* (MPa kg/m <sup>3</sup> )
PUR	150±6	0.75±0.02	8.14±0.03	0.0050	0.054
HPUR <sub>wca</sub>	170±4	0.39±0.03	7.28±0.02	0.0022	0.043
HPUR <sub>ca1</sub>	180±5	0.93±0.02	30.17±0.03	0.0052	0.168
HPUR <sub>ca2</sub>	190±6	2.15±0.04	50±0.09	0.011	0.263

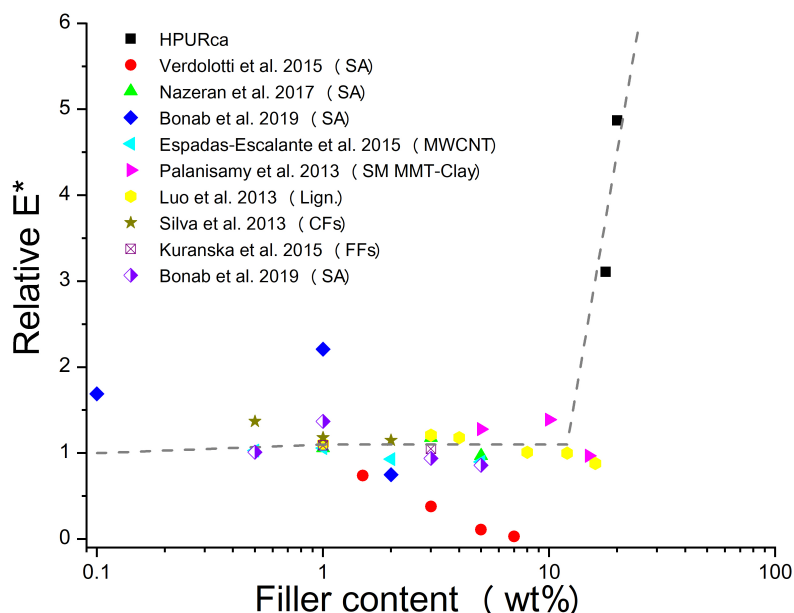


**Figure 8:** Relative ER\* (Young's Modulus normalised by bulk density relative to the pristine PUR foam in the same article) of polyurethane nanocomposite foams as a function of filler content. SA: Silica Aerogel [8, 17, 24], MWCNTs: Multiwall Carbon Nanotubes [36], SM MMT-Clay: Surface Modified Montmorillonite Clay [37], Lign.: Lignin [38], CFs: Cellulose Fibers [39], FFs: Flax Fibers [40] and PLNFs: Pineapple Leaf Nanofibers [41].

#### 4. Conclusions

The aim of this work was to enhance the performance of foamed PUR by modifying its nanostructure with the introduction of a nanoporous inorganic component. The resulting material is an organic-inorganic hybrid structure, obtained by incorporation of a precursor of a siloxane network during the foaming process and through a concomitant formation of the organic and inorganic interpenetrating networks. The siloxane network alone did not improve properties, a key role is played by the coupling agent, which bound the organic and inorganic phases, prevented siloxane aggregation and promoted formation of the interpenetrating organic-inorganic network. The hybrid structure is characterized by a multi-scale porosity (nano-micro), wherein the macro-porosity is given from the polyurethane phase, whereas the nano-porosity is given from the formation of aerogel-like siloxane domains. The hierarchical combination of these porosities allows a significant reduction of heat conductivity with respect to the pristine material. Moreover, the presence of the inorganic phase allowed improving the thermal degradation performances of the resulting hybrid material (so reducing or eliminating the need for flame retardants), as well as its mechanical

properties (i.e. modulus, strength, dimensional stability). In particular, the presence of “aerogel-like” polysiloxane structures with a content of 20 wt% in SiO<sub>2</sub>, HPUR<sub>ca2</sub>, induced a reduction of about 30% in thermal conductivity if compared with pristine PUR foam along with a significantly improvement in thermal stability and mechanical properties. In conclusion, the resulting hybrid materials exhibit an excellent balance between structural and functional properties and for this reason, it is a valuable candidate for substituting the traditional polymeric-based materials traditionally used in the thermal insulating of buildings and overcome the limitations which affect the widespread diffusion of silica aerogel materials.

## **Acknowledgments**

The work was supported by the PRIN project: SUSTAIN/ABLE- SimultaneoUs STructural And energetIc reNovAtion of BuiLdings through innovativE solutions. PE8LineaC-Prot. 20174RTL7W.

The authors are grateful to Fabio Docimo (CNR-IPCB), Mariarosaria Marcedula and Alessandra Aldi (CNR-IPCB) are kindly acknowledged for the technical support.

## **References**

- [1] Energy Efficiency Market Report 2014, IEA Paris, <https://doi.org/10.1787/9789264218260-en>.
- [2] Pavel CC, Blagoeva DT. Competitive landscape of the EU’s insulation materials industry for energy-efficient buildings EUR 28816 EN, Publications Office of the European Union, Luxembourg, 2018; ISBN 978-92-79-96383-4, doi:10.2760/750646, PUBSY No. JRC108692.

- [3] Villasmil W, Fischer LJ, Worlitschek J. A review and evaluation of thermal insulation materials and methods for thermal energy storage systems. *Renew Sustain Energy Rev* 2019; 10371–84.
- [4] Liu S, Zhu K, Cui S, Shen X, Tan G. A novel building material with low thermal conductivity: Rapid synthesis of foam concrete reinforced silica aerogel and energy performance simulation. *Energy Build* 2018; 177:385–393.
- [5]. Vareda JP, Lamy-Mendes A, Durães L. A reconsideration on the definition of the term aerogel based on current drying trends. *Microporous Mesoporous Mater* 2018; 258:211-216.
- [6] Karamikamkar S, Naguib HE, Park CB. Advances in precursor system for silica-based aerogel production toward improved mechanical properties, customized morphology, and multifunctionality: A review. *Adv Colloid Interface Sci.* 2020; 276:102101.
- [7] Kanamori K, Aizawa M, Nakanishi K, Hanada T. New Transparent Methylsilsesquioxane Aerogels and Xerogels with Improved Mechanical Properties. *Adv Mater* 2007; 19:1589-1593.
- [8] Bonaba SA, Moghaddasa J, Rezaei M. In-situ synthesis of silica aerogel/polyurethane inorganic-organic hybrid nanocomposite foams: Characterization, cell microstructure and mechanical properties. *Polymer* 2019; 172:27–40.
- [9] Kim YG, Kim HS, Jo SM, Kim SY. Thermally insulating, fire-retardant, smokeless and flexible polyvinylidene fluoride nanofibers filled with silica aerogels. *Chem Eng J* 2018; 351:473–481.
- [10] Kanamori K. Liquid-phase synthesis and application of monolithic porous materials based on organic–inorganic hybrid methylsiloxanes, crosslinked polymers and carbons. *J Sol-Gel Sci Technol* 2013;65:12–22.
- [11] Lakato Á. Investigation of the thermal insulation performance of fibrous aerogel samples under various hygrothermal environment: Laboratory tests completed with calculations and theory. *Energy Build* 2020; 214:109902.



- [12] Liu P, Yu H, Hui F, Villena MA, Li X, Lanza M, Zhang Z. Fabrication of 3D silica with outstanding organic molecule separation and self-cleaning performance. *Appl Surf Sci* 2020; 511:145537.
- [13] Yamasaki S, Sakuma W, Yasui H, Daicho K, Saito T, Fujisawa S, Isogai A, Kanamori K. Nanocellulose xerogels with high porosities and large specific surface areas. *Front Chem* 2019; 7:316.
- [14] Tallia F, Russo L, Li S, Orrin ALH, Shi X, Chen S, Steele JAM, Meille S, Chevalier J, Lee PD, Stevens MM, Cipolla L, Jones JR. Bouncing and 3D printable hybrids with self-healing properties, *Mater Horiz*, 2018; 5: 849-860.
- [15] Gama N, Costa LC; Amaral V, Ferreira A, Barros-Timmons A. Insights into the physical properties of biobased polyurethane/expanded graphite composite foams. *Compos Sci Technol* 2017; 138: 24-31.
- [16] Piscitelli F, Buonocore GG, Lavorgna M, Verdolotti L, Pricl S, Gentile G, Mascia L. Peculiarities in the structure – Properties relationship of epoxy-silica hybrids with highly organic siloxane domains. *Polymer* 2015; 63:222-229.
- [17] Verdolotti L, Lavorgna M, Lamanna R, Di Maio E, Iannace S. Polyurethane-silica hybrid foam by sol-gel approach: chemical and functional properties. *Polymer*, 2015; 56:20-28.
- [18] Piscitelli F, Lavorgna M, Buonocore GG, Verdolotti L, Galy J, Mascia L. Plasticizing and Reinforcing Features of Siloxane Domains in Amine-Cured Epoxy/Silica Hybrids. *Macromol Mater Eng* 2013; 298(8):896-909.
- [19] De Luca Bossa F, Santillo C, Verdolotti L, Campaner P, Minigher A, Boggioni L, Losio S, Coccia F, Iannace S, Lama GC. Greener Nanocomposite Polyurethane Foam Based on Sustainable Polyol and Natural Fillers: Investigation of Chemico-Physical and Mechanical Properties. *Materials* 2020; 13(1): 211.
- [20] Choe H, Lee JH, Kim JH. Polyurethane composite foams including CaCO<sub>3</sub> fillers for enhanced sound absorption and compression properties. *Compos. Sci. Technol.* 2020; 194: 1-6.
- [21] Lin S, Ionescu C, Pike KJ, Smith ME, Jones JR. Nanostructure evolution and calcium distribution in sol-gel derived bioactive glass. *J Mater Chem* 2009; 19:1276–1282.

- [22] Xu Y, Liu R, Wu D, Sun Y, Gao H, Yuan H, Deng F. Ammonia-catalyzed hydrolysis kinetics of mixture of tetraethoxysilane with methyltriethoxysilane by  $^{29}\text{Si}$  NMR. *J Non Cryst Solids* 2005; 351(30-32):2403-2413.
- [23] Pauw BR. Everything SAXS: small-angle scattering pattern collection and correction. *J Phys: Condens Matter* 2013; 25:383201.
- [24] Nazeran N., Moghaddas J. Synthesis and characterization of silica aerogel reinforced rigid polyurethane foam for thermal insulation application. *J Non Cryst Solids* 2017; 461:1-11.
- [25] Ema Y, Ikeya M, Okamoto M. Foam processing and cellular structure of polylactide-based nanocomposites. *Polymer* 2006; 47(15):5350-5359.
- [26] Verdolotti L, Lavorgna M, Di Maio E, Iannace S. Hydration-induced reinforcement of rigid polyurethane-cement foams: The effect of the co-continuous morphology on the thermal-oxidative stability. *Polym Deg Stability* 2013; 98(1):64-72.
- [27] Pau DSW, Fleischmann CM, Delichatsios MA. Thermal decomposition of flexible polyurethane foams in air. *Fire Saf J*, 2020; 111:102925.
- [28] Verdolotti L, Salerno A, Lamanna R, A. Nunziata, Netti P, Iannace S. A novel hybrid PU-alumina flexible foam with superior hydrophilicity and adsorption of carcinogenic compounds from tobacco smoke. *Microporous Mesoporous Mater* 2012; 151:79-87.
- [29] Zhao C, Yan Y, Hu Z, Li L, Fan X. Preparation and characterization of granular silica aerogel/polyisocyanurate rigid foam composites. *Constr Build Mater* 2015; 93:309-316.
- [30] Galzerano B, Capasso I, Verdolotti L, Lavorgna M, Vollaro P, Caputo D, Iannace S, Liguori B. Design of sustainable porous materials based on 3D-structured silica exoskeletons, Diatomite: Chemico-physical and functional properties. *Mater Des* 2018; 145:196-204.
- [31] Verdolotti L, Di Maio E, Lavorgna M, Iannace S. Hydration-induced reinforcement of rigid polyurethane-cement foams: mechanical and functional properties *J Mat Sci* 2012; 47(19):6948-6957.

- [32] Skochdopole RE. The thermal conductivity of foamed plastics. *Chem Eng Prog* 1961; 57:55-59.
- [33] Cao X, Lee LJ, Widya T, Macosko C. Polyurethane/clay nanocomposites foams: processing, structure and properties. *Polymer* 2005; 46(3): 75–783.
- [34] Nikje MMA, Tehrani ZM. Thermal and Mechanical Properties of Polyurethane Rigid Foam/Modified Nanosilica Composite. *Polym Eng Sci* 2010; 50(3):468-473.
- [35] Członka S, Strąkowska A, Strzelec K, Adamus-Włodarczyk A, Kairytė A, Vaitkus S. Composites of Rigid Polyurethane Foams Reinforced with POSS. *Polymers* 2019; 11(2):336.
- [36] Espadas-Escalante JJ, Avilés F. Anisotropic compressive properties of multiwall carbon nanotube/polyurethane foams. *Mech Mater* 2015; 91:167–176.
- [37] Palanismany A. Water-blown polyurethane–clay nanocomposite foams from biopolyol—effect of nanoclay on the properties. *Polym Compos* 2018; 34(8):1306-1312.
- [38] Luo X, Mohanty A, Misra M. Lignin as a reactive reinforcing filler for water-blown rigid biofoam composites from soy oil-based polyurethane. *Ind Crops Prod* 2013; 47:13– 19.
- [39] Silva MC, Takahashi JA, Chaussy D, Belgacem MN, Silva GG. Composites of rigid polyurethane foam and cellulose fiber residues. *J Appl Polym Sci* 2010; 117(6): 3665-3672.
- [40] Kurańska M, Prociak A. Flax fibers as natural filler for rigid polyurethane-polysocyanurate foams based on bio-polyol from rapeseed oil. *Tech Trans Chem* 2015; 1:47-54.
- [41] Zhou X, Wang H, Zhang J, Zheng Z, Du G. Lightweight Biobased Polyurethane Nanocomposites Foams Reinforced with Pineapple Leaf Nanofibers (PLNFs). *J Renew Mater* 2018; 6(1):68-74.